Hindawi Publishing Corporation
Mathematical Problems in Engineering
Volume 2011, Article ID 909410, 18 pages
doi:10.1155/2011/909410

Research Article

Mathematical Extrapolating of Highly Efficient Fin Systems

A.-R. A. Khaled

Thermal Engineering and Desalination Technology Department, King Abdulaziz University, P.O. Box 80204, Jeddah 21589, Saudi Arabia

Correspondence should be addressed to A.-R. A. Khaled, akhaled4@yahoo.com

Received 26 February 2011; Accepted 16 June 2011

Academic Editor: Bin Liu

Different high-performance fins are mathematically analyzed in this work. Initially, three types are considered: (i) exponential, (ii) parabolic, and (iii) triangular fins. Analytical solutions are obtained. Accordingly, the effective thermal efficiency and the effective volumetric heat dissipation rate are calculated. The analytical results were validated against numerical solutions. It is found that the triangular fin has the maximum effective thermal length. In addition, the exponential pin fin is found to have the largest effective thermal efficiency. However, the effective efficiency for the straight one is the maximum when its effective thermal length based on profile area is greater than 1.4. Furthermore, the exponential straight fin is found to have effective volumetric heat dissipation that can be 440% and 580% above the parabolic and triangular straight fins, respectively. In contrast, the exponential pin fin is found to possess effective volumetric heat dissipation that can be 120% and 132% above the parabolic and triangular pin fins, respectively. Finally, new high performance fins are mathematically generated that can have effective volumetric heat dissipation of 24% and 12% above those of exponential pin and straight fins, respectively.

1. Introduction

Fins are widely used in industry, especially in heat exchanger and refrigeration industries [1–5]. They are extended surfaces used to enhance heat transfer between the solids and the adjoining fluids [6]. Heat transfer inside fins has been extensively studied in the literature. Many mathematical analyses related to conduction and convection heat transfer in fins have been published. Harper and Brown [7] are considered the forerunner who began analyzing heat transfer inside fins mathematically. They found that one-dimensional analysis was sufficient for heat transfer inside fins. In addition, they recommended that tip heat loss can be accounted by using a corrected fin length which is equal to half of the fin thickness added to its length. Also, they pointed out that the differential surface area of the element is equal to the differential fin length element divided by the cosine of the taper angle.

Later on, Schmidt [8] analyzed mathematically longitudinal and radial fins of uniform thickness and longitudinal fins of trapezoidal profile. Many works have been followed before the work of Gardner [9]. He derived general mathematical solutions for the temperature excess profile and fin efficiency for fin satisfying the Murray [10] assumptions and whose thickness varies as some power of the distance from the fin tip. Gardner [9] work is considered an important work because he reemphasized the concept of fin efficiency. This concept has been used later on by thousands of works. In addition, he was one of the first to demonstrate the use of applied mathematics including the use of modified Bessel functions in conduction and convection heat transfer. Later on, many works used applied mathematics in analyzing heat transfer inside fins subject to variable convection heat transfer coefficient [11–13]. A sufficient and interesting literature about mathematical analysis in fin heat transfer is shown in the works of Kraus et al. [14] and Aziz and McFadden [15].

The fin thermal efficiency, η_f, is defined according to Gardner [9] as the fin heat transfer rate divided by the fin heat transfer rate if the fin surface is kept at uniform temperature of T_b. According to this definition, the fin efficiency depends on two independent factors: (i) fin thickness or radius distribution, and (ii) fin thermal length. Nowadays, it becomes a primary goal to improve the performance of thermal systems. This goal is obviously achievable by avoiding having fin thermal lengths more than its effective value. Owing to the fact that the fin effective thermal length is directly related to the fin profile [16], the fin efficiency can be improved and can be dependent only on the fin thickness or radius distribution. It should be noted that the fin effective thermal length is the one that produces fin heat transfer rate 1.0 percent below its maximum value. In this work, the fin efficiency based on the effective thermal length is named as the effective thermal efficiency. To the best knowledge of the author, almost negligible attention has been made towards analyzing high-performance fins based on their effective thermal efficiency. In addition, reducing the number of variables influencing the fin efficiency facilitates extrapolations of new generations of high-performance fins beyond those analyzed in the literature.

In this work, high-performance fins with effective thermal lengths are mathematically analyzed. Three types are initially considered: (i) exponential, (ii) parabolic, and (iii) triangular fins. Analytical forms for the excess temperature are obtained. As such, the fin effective thermal efficiency and the effective volumetric heat dissipation are calculated both analytically and numerically. Comparisons between the performances of each fin are performed. Finally, ultrahigh performance fin geometries are extrapolated from the derived solutions.

2. Problem Formulation

In this work, Murray [10] assumptions are considered. In addition, the square of the fin profile gradient is neglected.

2.1. Straight-Fins

Consider a rectangular fin having a thickness $H(x)$ that is much smaller than its length L as shown in Figure 1. $H(x)$ is considered to vary along the fin centerline axis (x-axis) according

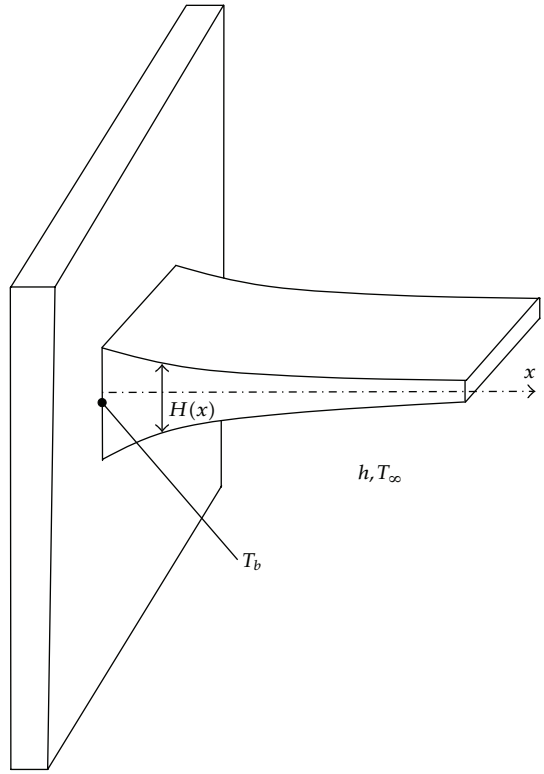

Figure 1: Schematic diagram for the straight fin and the system coordinate.

to the following relationships:

$$H(x) = H_b e^{-bx}, \tag{2.1}$$

$$H(x) = H_b\left(1 - \frac{x}{L}\right), \tag{2.2}$$

$$H(x) = H_b\left(1 - \frac{x}{L}\right)^2, \tag{2.3}$$

where b is a real positive number named as the exponential index. The quantity H_b represents the fin thickness at its base ($x = 0$). Equations (2.1)–(2.3) correspond to exponential, triangular, and parabolic straight fins, respectively.

The application of the energy equation [16] on a fin differential element results in the following differential equation:

$$\frac{d}{dx}\left(H\frac{dT}{dx}\right) - \frac{2h}{k}(T - T_\infty) = 0, \tag{2.4}$$

where T, T_∞, k, and h are the fin temperature, free stream temperature, fin thermal conductivity, and the convection heat transfer coefficient between the fin and the fluid stream,

respectively. The boundary conditions are the adiabatic tip conditions. Mathematically, they are given by

$$T(x=0)=T_b, \qquad \left.\frac{\partial T}{\partial x}\right|_{x=L_\infty}=0.0, \tag{2.5}$$

where L_∞ is the length that produces fin heat dissipation rate equal to 99 percent of the maximum heat dissipation rate.

2.1.1. Exponential Straight Fins

By solving (2.4) using (2.1), the following temperature distribution is obtained:

$$\frac{T(x)-T_\infty}{T_b-T_\infty}=e^{0.5bx}\left[\frac{K_0\left(2Xe^{0.5bL_\infty}\right)I_1\left(2Xe^{0.5bx}\right)+I_0\left(2Xe^{0.5bL_\infty}\right)K_1\left(2Xe^{0.5bx}\right)}{K_0\left(2Xe^{0.5bL_\infty}\right)I_1(2X)+I_0\left(2Xe^{0.5bL_\infty}\right)K_1(2X)}\right], \tag{2.6}$$

where $X=m/b$ and $m=\sqrt{2h/kH_b}$. The fin heat transfer rate per unit width for the exponential straight fin is calculated from

$$q_f'=-kH_b\left.\frac{dT}{dx}\right|_{x=0}=\sqrt{2hkH_b}(T_b-T_\infty)\left[\frac{I_0\left(2Xe^{0.5bL_\infty}\right)K_0(2X)-K_0\left(2Xe^{0.5bL_\infty}\right)I_0(2X)}{K_0\left(2Xe^{0.5bL_\infty}\right)I_1(2X)+I_0\left(2Xe^{0.5bL_\infty}\right)K_1(2X)}\right]. \tag{2.7}$$

The maximum heat transfer rate through exponential straight fins is obtained when considering L_∞ approaching infinity. It is equal to

$$\left(q_f'\right)_\infty=-kH_b\left.\frac{dT}{dx}\right|_{x=0}=\sqrt{2hk_fH_b}(T_b-T_\infty)\left[\frac{K_0(2X)}{K_1(2X)}\right]. \tag{2.8}$$

The effective thermal length mL_∞ is obtained by solving the equation given by $q_f'=0.99\left(q_f'\right)_\infty$. As such, the mL_∞ must satisfy the following relationship:

$$\frac{K_0\left(2Xe^{mL_\infty/2X}\right)}{I_0\left(2Xe^{mL_\infty/2X}\right)}=\frac{0.01K_0(2X)K_1(2X)}{I_0(2X)K_1(2X)+0.99I_1(2X)K_0(2X)}. \tag{2.9}$$

The fin thermal efficiency based on the fin effective thermal length is denoted by η_∞. Mathematically, it is equal to

$$\eta_\infty\equiv\frac{0.99\left(q_f'\right)_\infty}{2h(T_b-T_\infty)L_\infty}=\frac{0.99}{(mL_\infty)}\frac{K_0(2X)}{K_1(2X)}. \tag{2.10}$$

The fin dimensionless heat dissipation per unit effective thermal volume, β_∞, is defined as the ratio between the heat transfer rate through the fin of length L_∞ to maximum heat transfer

rate from a rectangular fin having the same base thickness and volume. Mathematically, it is equal to

$$\beta_\infty \equiv \frac{0.99\left(q_f'\right)_\infty}{(2h/H_b)(T_b - T_\infty)\int_0^{L_\infty} H\,dx} = \left(\frac{mL_\infty}{X}\right)\frac{\eta_\infty}{\left[1 - e^{-mL_\infty/X}\right]}. \tag{2.11}$$

It should be mentioned that the previous solutions could not be located in the literature.

2.1.2. Triangular Straight Fins

Equations (2.6)–(2.11) change to the following for the case of the triangular straight fin:

$$\frac{T(x) - T_\infty}{T_b - T_\infty} = \frac{K_1\left(2mL\sqrt{1 - L_\infty/L}\right)I_0\left(2mL\sqrt{1 - x/L}\right) + I_1\left(2mL\sqrt{1 - L_\infty/L}\right)K_0\left(2mL\sqrt{1 - x/L}\right)}{I_0(2mL)K_1\left(2mL\sqrt{1 - L_\infty/L}\right) + K_0(2mL)I_1\left(2mL\sqrt{1 - L_\infty/L}\right)}, \tag{2.12}$$

$$q_f' = \sqrt{2hkH_b}(T_b - T_\infty) \times \left[\frac{K_1\left(2mL\sqrt{1 - L_\infty/L}\right)I_1(2mL) - I_1\left(2mL\sqrt{1 - L_\infty/L}\right)K_1(2mL)}{I_0(2mL)K_1\left(2mL\sqrt{1 - L_\infty/L}\right) + K_0(2mL)I_1\left(2mL\sqrt{1 - L_\infty/L}\right)}\right], \tag{2.13}$$

$$\left(q_f'\right)_\infty = \sqrt{2hkH_b}(T_b - T_\infty)\left[\frac{I_1(2mL)}{I_0(2mL)}\right], \tag{2.14}$$

$$\frac{I_1\left(2mL\sqrt{1 - L_\infty/L}\right)}{K_1\left(2mL\sqrt{1 - L_\infty/L}\right)} = \frac{0.01I_0(2mL)I_1(2mL)}{I_0(2mL)K_1(2mL) + 0.99K_0(2mL)I_1(2mL)}, \tag{2.15}$$

$$\eta_\infty = \frac{0.99}{(mL_\infty)}\frac{I_1(2mL)}{I_0(2mL)} = 0.99\eta_f\left(\frac{mL}{mL_\infty}\right); \quad \eta_f \equiv \frac{\left(q_f'\right)_\infty}{2h(T_b - T_\infty)L_\infty}, \tag{2.16}$$

$$\beta_\infty = \frac{\eta_\infty}{[1 - (1/2)(mL_\infty/mL)]}, \tag{2.17}$$

where $m = \sqrt{2h/kH_b}$. It should be mentioned that (2.12)–(2.14) exist in different forms in the work of Kraus et al. [14].

2.1.3. Parabolic Straight Fins

Equations (2.6)–(2.11) change to the following for the case of the parabolic straight fin:

$$\frac{T(x)-T_\infty}{T_b-T_\infty}=\frac{(1-x/L)^{s_1}-(s_1/s_2)(1-L_\infty/L)^{s_1-s_2}(1-x/L)^{s_2}}{1-(s_1/s_2)(1-L_\infty/L)^{s_1-s_2}}, \tag{2.18}$$

$$q_f'=kH_b\left(\frac{s_1}{L}\right)(T_b-T_\infty)\left[\frac{1-(1-L_\infty/L)^{s_1-s_2}}{1-(s_1/s_2)(1-L_\infty/L)^{s_1-s_2}}\right], \tag{2.19}$$

$$\left(q_f'\right)_\infty=kH_b\left(\frac{s_2}{L}\right)(T_b-T_\infty), \tag{2.20}$$

$$\frac{(mL_\infty)}{(mL)}\cong 1-\left[\frac{1+\sqrt{1+4(mL)^2}}{199\sqrt{1+4(mL)^2}}\right]^{1/\sqrt{1+4(mL)^2}}, \tag{2.21}$$

$$\eta_\infty=\frac{0.99\times 2}{1+\sqrt{1+4(mL)^2}}\left(\frac{mL}{mL_\infty}\right)=0.99\eta_f\left(\frac{mL}{mL_\infty}\right);\qquad \eta_f\equiv\frac{\left(q_f'\right)_\infty}{2h(T_b-T_\infty)L}, \tag{2.22}$$

$$\beta_\infty=\frac{3\eta_\infty}{\left[1-(1-mL_\infty/[mL])^3\right]}\left(\frac{mL_\infty}{mL}\right), \tag{2.23}$$

where $m=\sqrt{2h/kH_b}$. The constants s_1 and s_2 are equal to the following:

$$s_1=-\frac{1}{2}-\frac{1}{2}\sqrt{1+4(mL)^2};\qquad s_2=-\frac{1}{2}+\frac{1}{2}\sqrt{1+4(mL)^2}. \tag{2.24}$$

It should be mentioned that (2.20) exists in a different form in the work of Kraus et al. [14].

2.2. Pin Fins

Consider a pin fin having a radius $r(x)$ that is much smaller than its length L as shown in Figure 2. $r(x)$ is taken to vary along the fin centerline axis (x-axis) according to the following relationships:

$$r(x)=r_be^{-bx}, \tag{2.25}$$

$$r(x)=r_b\left(1-\frac{x}{L}\right), \tag{2.26}$$

$$r(x)=r_b\left(1-\frac{x}{L}\right)^2, \tag{2.27}$$

where b is the exponential index. The quantity r_b represents the fin radius at its base ($x=0$). Equations (2.25)–(2.27) corresponds to exponential, triangular and parabolic pin-fins, respectively.

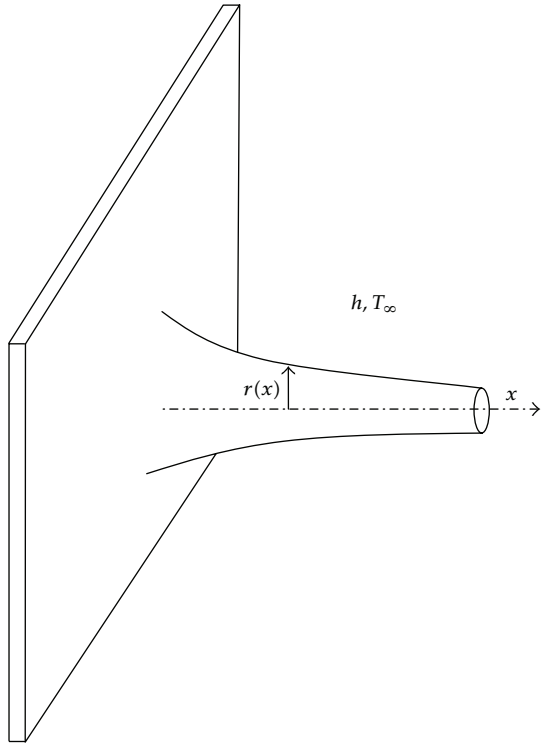

Figure 2: Schematic diagram for the pin fin and the system coordinate.

The application of the energy equation [16] on a fin differential element results in the following differential equation:

$$\frac{d}{dx}\left(r^2\frac{dT}{dx}\right) - \frac{2h}{k}r(T - T_\infty) = 0. \tag{2.28}$$

The boundary conditions are given by (2.5).

2.2.1. Exponential Pin Fins

By solving (2.28) using (2.25), the temperature distribution equals

$$\frac{T(x) - T_\infty}{T_b - T_\infty} = e^{bx}\left[\frac{K_1\left(2Xe^{0.5bL_\infty}\right)I_2\left(2Xe^{0.5bx}\right) + I_1\left(2Xe^{0.5bL_\infty}\right)K_2\left(2Xe^{0.5bx}\right)}{K_1\left(2Xe^{0.5bL_\infty}\right)I_2(2X) + I_1\left(2Xe^{0.5bL_\infty}\right)K_2(2X)}\right], \tag{2.29}$$

where $X = m/b$ and $m = \sqrt{2h/kr_b}$. The fin heat transfer rate is given by

$$q_f' = -k\pi r_b^2\left.\frac{dT}{dx}\right|_{x=0} = \pi r_b\sqrt{2hk_f r_b}(T_b - T_\infty)\left[\frac{K_1(2X)I_1\left(2Xe^{0.5bL_\infty}\right) - I_1(2X)K_1\left(2Xe^{0.5bL_\infty}\right)}{K_1\left(2Xe^{0.5bL_\infty}\right)I_2(2X) + I_1\left(2Xe^{0.5bL_\infty}\right)K_2(2X)}\right]. \tag{2.30}$$

The maximum heat transfer is obtained when L_∞ approaches infinity. It is equal to

$$\left(q_f'\right)_\infty = \pi r_b \sqrt{2hk_f r_b}(T_b - T_\infty)\left[\frac{K_1(2X)}{K_2(2X)}\right]. \tag{2.31}$$

The effective thermal length mL_∞ is obtained when $q_f' = 0.99(q_f')_\infty$. As such, it can be obtained by solving the following equation:

$$\frac{K_1\left(2Xe^{mL_\infty/2X}\right)}{I_1\left(2Xe^{mL_\infty/2X}\right)} = \frac{0.01K_1(2X)K_2(2X)}{I_1(2X)K_2(2X) + 0.99I_2(2X)K_1(2X)}. \tag{2.32}$$

The fin effective thermal efficiency for the exponential pin fin is equal to

$$\eta_\infty \equiv \frac{0.99\left(q_f'\right)_\infty}{2\pi h(T_b - T_\infty)\int_0^{L_\infty} r\,dx} = \frac{0.99}{X\left(1 - e^{-mL_\infty/X}\right)}\frac{K_1(2X)}{K_2(2X)} = \frac{0.99\eta_f}{\left(1 - e^{-mL_\infty/X}\right)}. \tag{2.33}$$

The fin dimensionless heat transfer per unit effective volume β_∞, is defined here as the ratio between the heat transfer rate of the fin with length L_∞ to maximum heat transfer rate from a rectangular pin fin having the same base radius and volume. Mathematically, it is equal to

$$\beta_\infty \equiv \frac{0.99\left(q_f'\right)_\infty}{(2\pi h/r_b)(T_b - T_\infty)\int_0^{L_\infty} r^2\,dx} = \frac{2\eta_\infty}{\left[1 + e^{-mL_\infty/X}\right]}. \tag{2.34}$$

It should be mentioned that (2.29)–(2.34) could not be located in the literature at least in the same form as they are shown.

2.2.2. Triangular Pin Fins

Equations (2.29)–(2.34) change to the following for the case of the triangular pin fin:

$$\begin{aligned}\frac{T(x) - T_\infty}{T_b - T_\infty} = {} & \frac{[1 - x/L]^{-0.5}K_2\left(2mL[1 - L_\infty/L]^{0.5}\right)I_1\left(2mL[1 - x/L]^{0.5}\right)}{I_1(2mL)K_2\left(2mL[1 - L_\infty/L]^{0.5}\right) + K_1(2mL)I_2\left(2mL[1 - L_\infty/L]^{0.5}\right)} \\ & + \frac{[1 - x/L]^{-0.5}I_2\left(2mL[1 - L_\infty/L]^{0.5}\right)K_1\left(2mL[1 - x/L]^{0.5}\right)}{I_1(2mL)K_2\left(2mL[1 - L_\infty/L]^{0.5}\right) + K_1(2mL)I_2\left(2mL[1 - L_\infty/L]^{0.5}\right)},\end{aligned} \tag{2.35}$$

$$q_f' = \pi r_b \sqrt{2hkr_b}(T_b - T_\infty) \times \left[\frac{K_2\left(2mL[1 - L_\infty/L]^{0.5}\right)I_2(2mL) - I_2\left(2mL[1 - L_\infty/L]^{0.5}\right)K_2(2mL)}{K_2\left(2mL[1 - L_\infty/L]^{0.5}\right)I_1(2mL) + I_2\left(2mL[1 - L_\infty/L]^{0.5}\right)K_1(2mL)}\right], \tag{2.36}$$

$$\left(q_f'\right)_\infty = \pi r_b \sqrt{2hkr_b}(T_b - T_\infty)\left[\frac{I_2(2mL)}{I_1(2mL)}\right], \tag{2.37}$$

$$\frac{I_2\left(2mL[1 - L_\infty/L]^{0.5}\right)}{K_2\left(2mL[1 - L_\infty/L]^{0.5}\right)} = \frac{0.01I_1(2mL)I_2(2mL)}{K_2(2mL)I_1(2mL) + 0.99I_2(2mL)K_1(2mL)}, \tag{2.38}$$

$$\eta_\infty = \frac{0.99}{(mL_\infty)[1 - 0.5(mL_\infty/[mL])]}\frac{I_2(2mL)}{I_1(2mL)} = 0.99\eta_f \frac{(mL/[mL_\infty])^2}{[2(mL/[mL_\infty]) - 1]}, \tag{2.39}$$

$$\beta_\infty = \frac{3\eta_\infty(L_\infty/L)[1 - 0.5(L_\infty/L)]}{\left[1 - (1 - [L_\infty/L])^3\right]}, \tag{2.40}$$

where $m = \sqrt{2h/kr_b}$. It should be mentioned that (2.37) matches a solution shown in [16].

2.2.3. Parabolic Pin Fins

Equations (2.29)–(2.34) change to the following for the case of parabolic pin fin:

$$\frac{T(x) - T_\infty}{T_b - T_\infty} = \frac{(1 - (x/L))^{p_1} - (p_1/p_2)(1 - (L_\infty/L))^{p_1 - p_2}(1 - (x/L))^{p_2}}{1 - (p_1/p_2)(1 - (L_\infty/L))^{p_1 - p_2}}, \tag{2.41}$$

$$q_f' = k\pi r_b^2\left(\frac{p_1}{L}\right)(T_b - T_\infty)\left[\frac{1 - (1 - (L_\infty/L))^{p_1 - p_2}}{1 - (p_1/p_2)(1 - (L_\infty/L))^{p_1 - p_2}}\right], \tag{2.42}$$

$$\left(q_f'\right)_\infty = k\pi r_b^2\left(\frac{p_2}{L}\right)(T_b - T_\infty), \tag{2.43}$$

$$\frac{(mL_\infty)}{(mL)} \cong 1 - \left[\frac{1 + \sqrt{1 + (4/9)(mL)^2}}{199\sqrt{1 + (4/9)(mL)^2}}\right]^{1/[3\times\sqrt{1+(4/9)(mL)^2}]}, \tag{2.44}$$

$$\eta_\infty = \frac{0.99 \times 9}{2(mL)^2\left[1 - (1 - mL_\infty/(mL))^3\right]}\left[\sqrt{1 + \frac{4}{9}(mL)^2} - 1\right] = \frac{0.99\eta_f}{\left[1 - (1 - mL_\infty/(mL))^3\right]}, \tag{2.45}$$

$$\beta_\infty = \frac{5\eta_\infty\left[1 - (1 - [L_\infty/L])^3\right]}{3\left[1 - (1 - [L_\infty/L])^5\right]}, \tag{2.46}$$

where $m = \sqrt{2h/kr_b}$. The constants p_1 and p_2 are equal to the following:

$$p_1 = -\frac{3}{2} - \frac{3}{2}\sqrt{1 + \frac{4}{9}(mL)^2}, \qquad p_2 = -\frac{3}{2} + \frac{3}{2}\sqrt{1 + \frac{4}{9}(mL)^2}. \tag{2.47}$$

It should be mentioned that (2.43) matches with a solution shown in [16].

2.3. Generation of High-performance Fins

2.3.1. High-Order Polynomial Method

The variation of the high-performance fin profile with its β_∞-indicator can be approximated by the following relationship:

$$\frac{r(x)}{r_b} = \frac{H(x)}{H_b} \cong 1 + b(x)\beta_\infty + c(x)\beta_\infty^2 + d(x)\beta_\infty^3, \tag{2.48}$$

where the coefficients $b(x)$, $c(x)$, and $d(x)$ should satisfy the following conditions:

$$1 - \left(\frac{x}{L}\right) \cong 1 + b(x)\left[(\beta_\infty)_t\right] + c(x)\left[(\beta_\infty)_t\right]^2 + d(x)\left[(\beta_\infty)_t\right]^3, \tag{2.49}$$

$$\left[1 - \left(\frac{x}{L}\right)\right]^2 \cong 1 + b(x)\left[(\beta_\infty)_p\right] + c(x)\left[(\beta_\infty)_p\right]^2 + d(x)\left[(\beta_\infty)_p\right]^3, \tag{2.50}$$

$$e^{-bx} \cong 1 + b(x)\left[(\beta_\infty)_e\right] + c(x)\left[(\beta_\infty)_e\right]^2 + d(x)\left[(\beta_\infty)_e\right]^3. \tag{2.51}$$

The quantities $(\beta_\infty)_t$, $(\beta_\infty)_p$, and $(\beta_\infty)_e$ are the corresponding β_∞-values of triangular, parabolic, and exponential fins, respectively. Solving (2.49)–(2.51) for the functions $b(x)$, $c(x)$, and $d(x)$ and rearranging (2.48), the following equation can be obtained:

$$\begin{aligned}\frac{r(x)}{r_b} = \frac{H(x)}{H_b} \cong 1 &+ \frac{\beta_\infty\left[\beta_\infty - (\beta_\infty)_t\right]\left|\beta_\infty - (\beta_\infty)_p\right|}{(\beta_\infty)_e\left[(\beta_\infty)_e - (\beta_\infty)_t\right]\left[(\beta_\infty)_e - (\beta_\infty)_p\right]}\left\{e^{-mx/X} - 1\right\} \\ &+ \frac{\beta_\infty\left[\beta_\infty - (\beta_\infty)_t\right]\left[\beta_\infty - (\beta_\infty)_e\right]}{(\beta_\infty)_p\left[(\beta_\infty)_p - (\beta_\infty)_t\right]\left[(\beta_\infty)_p - (\beta_\infty)_e\right]}\left\{\left[1 - \frac{mx}{mL_p}\right]^2 - 1\right\} \\ &+ \frac{\beta_\infty\left[\beta_\infty - (\beta_\infty)_p\right]\left[\beta_\infty - (\beta_\infty)_e\right]}{(\beta_\infty)_t\left[(\beta_\infty)_t - (\beta_\infty)_p\right]\left[(\beta_\infty)_t - (\beta_\infty)_e\right]}\left\{-\frac{mx}{mL_t}\right\}, \quad 0 \le mx \le mL_t,\end{aligned} \tag{2.52}$$

where mL_t, mL_p, and X are obtained by solving (2.9), (2.15), (2.21), (2.32), (2.38), and (2.44) at the same mL_∞ that is used to obtain $(\beta_\infty)_t$, $(\beta_\infty)_p$, and $(\beta_\infty)_e$. Practically, (2.52) can be used as long as positive fin thicknesses or radii are produced.

2.3.2. Exponential Method

The variation of the high-performance fin profile with its β_∞-indicator can be approximated by the following relationship:

$$\frac{r(x)}{r_b} = \frac{H(x)}{H_b} \cong 1 + i(x)\left(\beta_\infty\right)^{j(x)} e^{-l(x)\beta_\infty}, \quad 0 \le mx \le mL_t, \tag{2.53}$$

where the coefficients $i(x)$, $j(x)$, and $l(x)$ should satisfy the following conditions:

$$1 - \left(\frac{x}{L}\right) \cong 1 + i(x)\left[\left(\beta_\infty\right)_t\right]^{j(x)} e^{-l(x)\left[\left(\beta_\infty\right)_t\right]}, \tag{2.54}$$

$$\left[1 - \left(\frac{x}{L}\right)\right]^2 \cong 1 + i(x)\left[\left(\beta_\infty\right)_p\right]^{j(x)} e^{-l(x)\left[\left(\beta_\infty\right)_p\right]}, \tag{2.55}$$

$$e^{-bx} \cong 1 + i(x)\left[\left(\beta_\infty\right)_e\right]^{j(x)} e^{-l(x)\left[\left(\beta_\infty\right)_e\right]}. \tag{2.56}$$

The quantities $\left(\beta_\infty\right)_t$, $\left(\beta_\infty\right)_p$, and $\left(\beta_\infty\right)_e$ are the corresponding β_∞-values of triangular, parabolic and exponential fins, respectively. Solving (2.54)–(2.56) for the functions $i(x)$, $j(x)$, and $l(x)$, the following equations are obtained:

$$j(x) = \frac{\ln\left[\dfrac{\left(e^{-mx/X} - 1\right)}{\left(-mx/[mL_t]\right)}\right] - \left\{\dfrac{\left(\beta_\infty\right)_e - \left(\beta_\infty\right)_t}{\left(\beta_\infty\right)_p - \left(\beta_\infty\right)_t}\right\} \ln\left[\dfrac{\left(1 - (mx)/[mL_p]\right)^2 - 1}{-mx/[mL_t]}\right]}{\ln\left[\dfrac{\left(\beta_\infty\right)_e}{\left(\beta_\infty\right)_t}\right] - \left\{\dfrac{\left(\left(\beta_\infty\right)_e - \left(\beta_\infty\right)_t\right)}{\left(\left(\beta_\infty\right)_p - \left(\beta_\infty\right)_t\right)}\right\} \ln\left[\dfrac{\left(\beta_\infty\right)_p}{\left(\beta_\infty\right)_t}\right]}, \tag{2.57}$$

$$l(x) = \frac{\ln\left[\dfrac{\left(\beta_\infty\right)_p}{\left(\beta_\infty\right)_t}\right] / \ln\left[\dfrac{\left(\beta_\infty\right)_e}{\left(\beta_\infty\right)_t}\right] \ln\left[\dfrac{\left(e^{-mx/X} - 1\right)}{\left(-mx/[mL_t]\right)}\right] - \ln\left[\dfrac{\left(1 - (mx)/[mL_p]\right)^2 - 1}{-mx/[mL_t]}\right]}{\left\{\left(\beta_\infty\right)_p - \left(\beta_\infty\right)_t\right\} - \left\{\left(\beta_\infty\right)_e - \left(\beta_\infty\right)_t\right\} \ln\left[\dfrac{\left(\beta_\infty\right)_p}{\left(\beta_\infty\right)_t}\right] / \ln\left[\dfrac{\left(\beta_\infty\right)_e}{\left(\beta_\infty\right)_t}\right]}, \tag{2.58}$$

$$i(x) = -\left(\frac{mx}{mL_t}\right)\left[\left(\beta_\infty\right)_t\right]^{-j(x)} e^{l(x)\left(\beta_\infty\right)_t}, \tag{2.59}$$

where mL_t, mL_p, and X are obtained by solving (2.9), (2.15), (2.21), (2.32), (2.38) and (2.44) at the same mL_∞ that is used to obtain $\left(\beta_\infty\right)_t$, $\left(\beta_\infty\right)_p$, and $\left(\beta_\infty\right)_e$. Also, (2.53) can be used as long as positive fin thicknesses or radii are produced.

3. Numerical Methodology

Equations (2.4) and (2.28) were descretized using three points central differencing according to the following equations:

$$\begin{aligned}\overline{H}_{i-1/2}\theta_{i-1} - \left[\overline{H}_{i+1/2} + \overline{H}_{i-1/2} + (mL)^2\Delta\overline{x}^2\right]\theta_i + \overline{H}_{i+1/2}\theta_{i+1} = 0,\\ (\overline{r}_{i-1/2})^2\theta_{i-1} - \left[(\overline{r}_{i+1/2})^2 + (\overline{r}_{i-1/2})^2 + (mL)^2\overline{r}_i\Delta\overline{x}^2\right]\theta_i + (\overline{r}_{i+1/2})^2\theta_{i+1} = 0,\end{aligned} \tag{3.1}$$

where i is the location of the descretized point in the $\overline{x}$ direction. $\overline{x}$, $\overline{H}$, $\overline{r}$, and θ are the dimensionless forms of x, H, r, and T, respectively. The resulting tridiagonal systems of algebraic equations shown by (3.1) were solved using the well-established Thomas algorithm (Blottner [17]). The integrals shown in (2.11), (2.33), and (2.34) were computed numerically using the Simpson's rule [18]. Table 1 shows comparisons between the numerical and the analytical results of the effective efficiency. Excellent agreement is noticed in this table. As such, this led to more confidence in the obtained analytical solutions.

3.1. Useful Correlations

The results generated by solving (2.9), (2.15), (2.32), and (2.38) are shown in form of correlations, which were developed using well-known software. The correlations have the following functional form:

$$\Pi = \frac{g_1\Phi^{g_2} + g_3\Phi^{g_4} + g_5\Phi^{g_6}}{g_7\Phi^{g_8} + g_9\Phi^{g_{10}} + g_{11}\Phi^{g_{12}}}. \tag{3.2}$$

The correlation constants g_1–g_{12} for the different studied cases are listed in Table 2. Maximum errors associated with these correlations are less than 1% for all used ranges of mL and when $X > 0.015$.

4. Discussion of the Results

Figures 3 and 4 illustrate the variation of the effective efficiency and efficiency ratio η_∞/η_f with the fin thermal length mL. These figures show that thermal efficiencies of parabolic, triangular, and exponential fins can be significantly increased especially at large thermal lengths. This is achievable by eliminating the fin portions beyond the effective thermal length mL_∞. Triangular pin fins are found to possess larger η_∞/η_f-values than parabolic pin fins. However, parabolic straight fins have always larger η_∞/η_f-values than triangular straight fins. It should be noted that fin volumes near the tip are maximum for triangular fins. As a consequence, triangular fins have always larger effective thermal lengths than exponential and parabolic fins. This fact can be noticed from Figures 3 and 4 along with (2.16), (2.22), (2.33), (2.39), and (2.45).

Figure 5 shows the relation between the effective thermal efficiency η_∞ and the effective thermal length $L_\infty^{3/2}(h/kA_{p\infty})^{1/2}$ based on the effective profile area, $A_{p\infty}$, for the different types of the straight fins. It should be noted that

Table 1: Comparisons between the numerical and the analytical results.

Fin type	Thermal condition	Numerical computation of η_∞	Analytical computation of η_∞	Percent difference
Straight-triangular	$mL = 2.5$	0.4703	0.4704	0.02%
Straight-parabolic	$mL = 2.0$	0.5457	0.5459	0.04%
Straight-exponential	$X = 2.0$	0.4414	0.4419	0.1%
Pin-triangular	$mL = 1.5$	0.7753	0.7756	0.04%
Pin-parabolic	$mL = 1.0$	0.9174	0.9178	0.04%
Pin-exponential	$X = 2.0$	0.5763	0.5764	0.02%

Table 2: Correlation constants, see (3.2), for the analyzed straight fins.

Coefficient	Triangular straight $\Pi = mL_\infty$ $\Phi = mL$	Triangular straight $\Pi = mL$ $\Phi = mL_\infty$	Exponential straight $\Pi = mL_\infty$ $\Phi = X$	Triangular Pin $\Pi = mL_\infty$ $\Phi = mL$	Triangular Pin $\Pi = mL$ $\Phi = mL_\infty$	Exponential straight $\Pi = mL_\infty$ $\Phi = X$
g_1	0.69428	598.742	3.8343	1.46608	7.27154	0.931451
g_2	−1.98283	−7.1912	−0.894435	0.117199	0.311742	−0.514116
g_3	0.198954	12.3343	7.0634	4.2461	−0.546715	4.46038
g_4	−1.76853	−2.80184	−0.274186	−1.98447	4.10486	0.513971
g_5	0.167474	2.12319	0.208524	−0.578418	0.40409	−5.04956
g_6	1.06061	0.746752	−0.131276	0.116989	4.33523	0.523092
g_7	0.886024	588.714	0.704077	0.973387	−0.389977	0.119439
g_8	−2.9514	−8.19517	−1.7562	−1.29981	2.18417	−0.367153
g_9	0.141659	3.82157	3.17823	4.63058	4.673	0.105864
g_{10}	0.623454	−1.09171	−1.10017	−2.99168	−0.699218	−1.22631
g_{11}	0.0680181	−0.0615233	2.84166	0.33941	1.77476	0.000821297
g_{12}	1.04416	3.2981	−0.273702	0.116343	−0.695973	0.483324

$L_\infty^{3/2}(h/kA_{p\infty})^{1/2}$ is equal to $mL_\infty\sqrt{[2 - L_\infty/L]^{-1}}$, $mL_\infty\sqrt{1.5(L_\infty/L)[1 - (1 - L_\infty/L)^3]^{-1}}$, and $(mL_\infty)^{3/2}\sqrt{[2X(1 - e^{-mL_\infty/X})]^{-1}}$ for triangular, parabolic and exponential straight fins, respectively. Figure 5 shows that the triangular straight fin has the maximum η_∞-value when $L_\infty^{3/2}(h/kA_{p\infty})^{1/2} < 0.95$. However, the exponential straight fin possesses the maximum η_∞-value when $L_\infty^{3/2}(h/kA_{p\infty})^{1/2} \geq 1.4$. Exponential pin fins have the maximum effective thermal efficiency for the same effective thermal length, mL_∞, as shown from Figure 6. The variation of η_∞ with the fin geometry is almost insignificant for the analyzed pin fins. Figures 5 and 6 demonstrate that the minimum effective thermal efficiency for all fins is 0.377.

Exponential fins have the largest effective heat dissipation per unit volume, β_∞, as evident from Figures 7 and 8 while triangular fins have the smallest β_∞-values. All of the analyzed fins are noticed to have an asymptotic β_∞-value of 0.375 as their thermal lengths approaches infinity. Figures 9 and 10 show a number of fin-geometries having high thermal performances. The pin fin geometry with $\beta_\infty = 1.83$ has volumetric heat dissipation 17% above that of the exponential pin fin. The exact β_∞-value of that plot is 1.795 which deviates

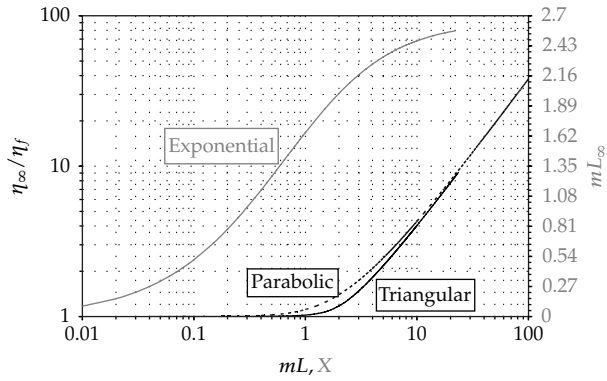

Figure 3: Effects of the fin dimensionless length X and thermal length mL on the effective thermal length mL_∞ for exponential straight fin and the maximum available efficiency ratio η_∞/η_f for triangular and parabolic straight fins, $m = \sqrt{2h/kH_b}$.

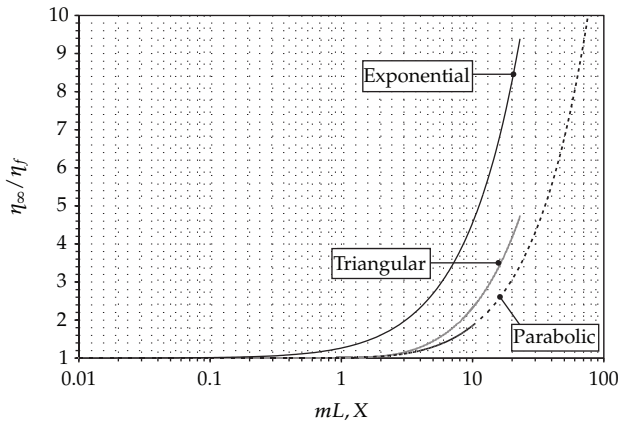

Figure 4: Effects of the fin dimensionless length X and thermal length mL on the maximum available efficiency ratio η_∞/η_f for exponential, triangular and parabolic pin fins, $m = \sqrt{2h/kr_b}$.

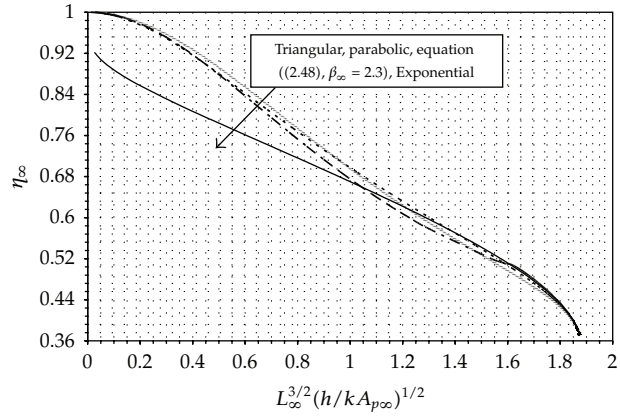

Figure 5: Effect of the fin effective thermal length based on profile area on the fin effective thermal efficiency η_∞ for exponential, parabolic, and triangular straight fins, $m = \sqrt{2h/kH_b}$.

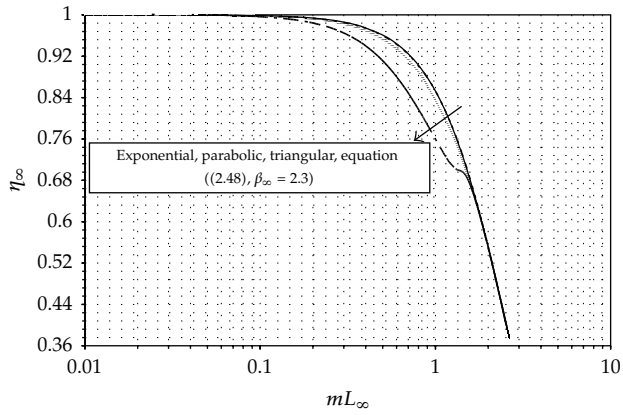

Figure 6: Effect of the fin minimum effective thermal mL_∞ on the fin efficiency η_f for exponential, parabolic, and triangular pin fins, $m = \sqrt{2h/kr_b}$.

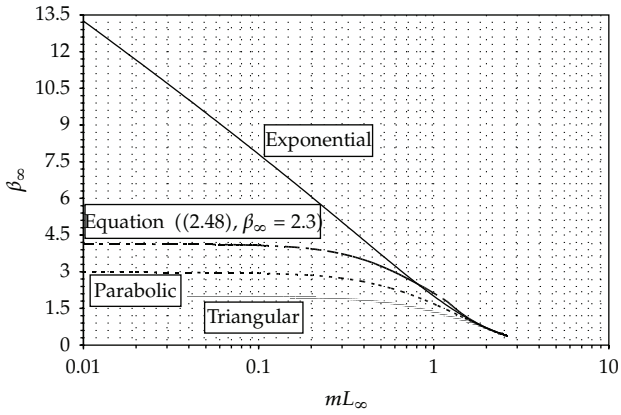

Figure 7: Effect of the fin minimum effective thermal length mL_∞ on β_∞ for exponential, parabolic, and triangular straight fins, $m = \sqrt{2h/kH_b}$.

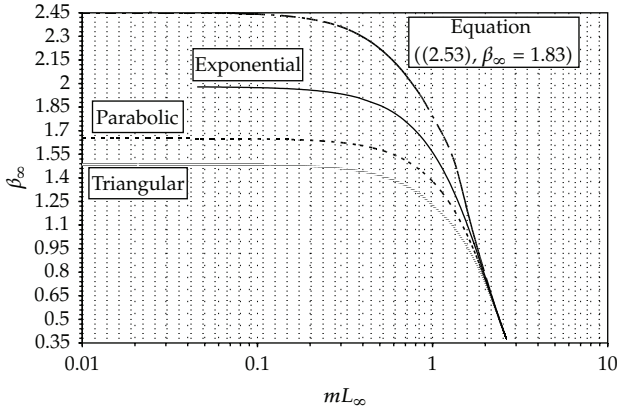

Figure 8: Effect of the fin minimum effective thermal length mL_∞ on β_∞ for exponential, parabolic, and triangular pin fins, $m = \sqrt{2h/kr_b}$.

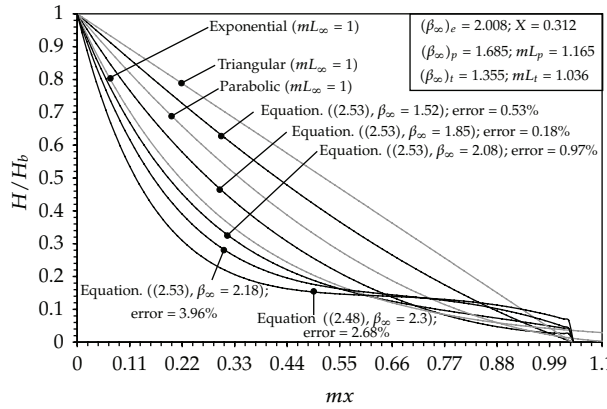

Figure 9: New high-performance straight fins profiles, $m = \sqrt{2h/kH_b}$.

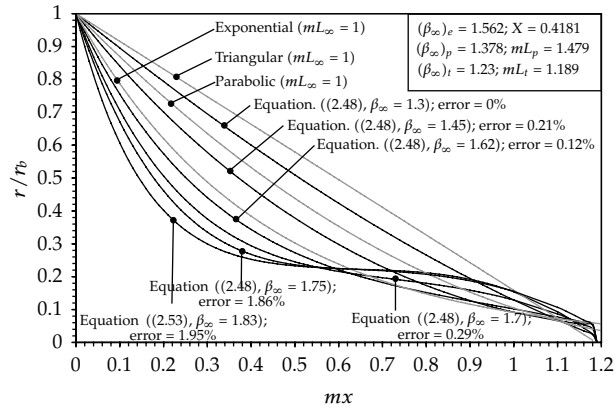

Figure 10: New high-performance pin fins profiles, $m = \sqrt{2h/kr_b}$.

from the estimated value, $\beta_\infty = 1.83$, by 1.95%. It is noticed from Figures 9 and 10 that errors associated with (2.53) are smaller than those associated with (2.52). The effective thermal efficiency of the fin shown by (2.52) with $\beta_\infty = 2.3$ is larger than that of the exponential fin at smaller effective thermal lengths while its effective volumetric heat dissipation is larger than that of exponential fin when $mL_\infty > 0.5$ as shown in Figures 5 and 7. Figure 8 shows that the pin fin with profile given by (2.53) with $\beta_\infty = 1.83$ possesses maximum volumetric heat dissipation that is 24% above that of the exponential pin fin.

5. Conclusions

Heat transfer through high-performance fins was mathematically analyzed under conditions that lead to useful thermal lengths. Three fin types were considered: parabolic, triangular, and exponential straight or pin fins. Analytical solutions were obtained. The effective thermal length was obtained for each case. Accordingly, the effective thermal efficiency and the effective heat dissipation per unit volume were calculated. The analytical results were

compared against numerical solutions and excellent agreements were found. The following remarks were concluded:

(i) Triangular fins have always-larger effective thermal lengths than parabolic fins.

(ii) Exponential pin fins possess the largest effective thermal efficiencies.

(iii) The exponential straight fin possesses the maximum effective thermal efficiency when its effective thermal length based on profile area is greater than 1.4.

(iv) The triangular straight fin has the maximum effective thermal efficiency when its effective thermal length based on profile area is smaller than 0.95.

(v) Exponential straight fins were found to possess effective volumetric heat dissipation that can be 440% and 580% above parabolic and triangular straight fins.

(vi) Exponential pin fins were found to possess effective volumetric heat dissipation that can be 120% and 132% above parabolic and triangular pin fins.

(vii) The derived analytical solutions were used to generate new high-performance fins that possess volumetric heat dissipation 24% and 12% above those of exponential pin and straight fins, respectively.

Nomenclature

$A_{p\infty}$: Effective fin profile area
b: Exponential functions indices
H: Fin thickness
H_b: Tin thickness at its base
h: Convection heat transfer coefficient
$I_n(x)$: Modified Bessel functions of the first kind of order n
$K_n(x)$: Modified Bessel functions of the second kind of order n
k: Fin thermal conductivity
L: Fin length
L_∞: Effective fin length
m: Fin thermal index
q'_f: Fin heat transfer rate per unit width
$(q'_f)_\infty$: Maximum fin heat transfer rate per unit width
r: Fin radius
r_b: Fin radius at its base
T: Fin temperature
T_b: Fin base temperature
T_∞: Free stream temperature of the adjoining fluid
V_f: Fin volume
X: Dimensionless exponential fin parameter
x: Coordinate axis along the fin centreline.

Greek Symbols

β_∞: Fin effective dimensionless volumetric heat dissipation
η_f: Fin thermal efficiency
η_∞: Fin effective thermal efficiency.

Acknowledgment

The support of this work by King Abdulaziz City for Science and Technology (KACST) under Project no. 8-ENE192-3 is acknowledged.

References

[1] A. E. Bergles, "The implications and challenges of enhanced heat transfer for the chemical process industries," *Chemical Engineering Research and Design*, vol. 79, no. 4, pp. 437–434, 2001.
[2] E. I. Nesis, A. F. Shatalov, and N. P. Karmatskii, "Dependence of the heat transfer coefficient on the vibration amplitude and frequency of a vertical thin heater," *Journal of Engineering Physics and Thermophysics*, vol. 67, no. 1-2, pp. 696–698, 1994.
[3] J. K. Hagge, G. H. Junkhan et al., "Experimental study of a method of mechanical augmentation of convective heat transfer in air," Tech. Rep. HTL3, ISU-ERI-Ames-74158, Iowa State University, The Netherlands, 1975.
[4] W. M. Kays, "Pin-fin heat-exchanger surfaces," *Journal of Heat Transfer of the American Society of Mechanical Engineers*, vol. 77, pp. 471–483, 1955.
[5] D. O. Kern and A. D. Kraus, *Extended Surface Heat Transfer*, McGraw-Hill, New York, NY, USA, 1972.
[6] A. E. Bergles, *Handbook of Heat Transfer*, McGraw-Hill, New York, NY, USA, 3rd edition, 1998.
[7] D. R Harper and W. B. Brown, "Mathematical equations for heat conduction in the fins of air cooled engines," Tech. Rep. NACA Rep. 158, National Committee on Aeronutics, Washington, DC, USA, 1922.
[8] E. Schmidt, "Die Wärmeűberagung durch Rippen," *Zeitschrift Des Vereines Deutscher Ingenieure*, vol. 70, pp. 885–947, 1926.
[9] K. A. Gardner, "Efficiency of extended surface," *Transactions of the American Society of Mechanical Engineers*, vol. 67, p. 621, 1945.
[10] W. M. Murray, "Heat transfer through an annular disk or fin of uniform thickness," *Transactions of the American Society of Mechanical Engineers, Journal of Applied Mechanics*, vol. 60, p. 78, 1938.
[11] L. S. Han and S. G. Lefkowitz, "Constant cross section fin efficiencies for non-uniform surface heat transfer coefficients," Tech. Rep. 60-WA-41, American Society of Mechanical Engineers, New York, NY, USA, 1960.
[12] S. Y. Chen and G. L. Zyskowski, "Steady state heat conduction in a straight fin with variable heat transfer coefficient," in *Proceedings of the 6th National heat transfer conference*, no. 63-HT-1, American Society of Mechanical Engineers, Boston, Mass, USA, 1963.
[13] L. I. Roizen, "Heat transfer in flow round straight transverse fins," *Inzhenerno-Fizicheskii Zhurnal*, vol. 11, no. 2, p. 148, 1966.
[14] A. D. Kraus, A. Aziz, and J. R. Welty, *Extended Surface Heat Transfer*, John Wiley & Sons, New York, NY, USA, 2001.
[15] A. Aziz and G. McFadden, "Some new solutions for extended surface heat transfer using symbolic algebra," *Heat Transfer Engineering*, vol. 26, no. 9, pp. 30–40, 2005.
[16] F. P. Incorpera, D. P. DeWitt, T. L. Bergman, and A. S. Lavine, *Fundamentals of Heat and Mass Transfer*, John Wiley & Sons, New York, NY, USA, 6th edition, 2006.
[17] F. G. Blottner, "Finite-difference methods of solution of the boundary-layer equations," *American Institute of Aeronautics and Astronautics Journal*, vol. 8, pp. 193–205, 1970.
[18] M. R. Spiegel, *Mathematical Handbook of Formulas and Tables*, McGraw-Hill, New York, NY, USA, 1990.